

Modification of the spin structure of chromium by an interface effect in Cr(011)/Sn multilayers

N. Jiko*

Institute for Chemical Research, Kyoto University, Uji, Kyoto 611-0011, Japan

K. Mibu

Research Center for Low Temperature and Materials Sciences, Kyoto University, Uji, Kyoto 611-0011, Japan

M. Takeda

Advanced Science Research Center, Japan Atomic Energy Research Institute, Tokai, Ibaraki 319-1195, Japan

(Received 7 July 2004; revised manuscript received 10 September 2004; published 12 January 2005)

We have studied the magnetic structure of Cr layers in Cr(011)/Sn multilayers, where monatomic Sn layers are periodically inserted along the bcc [011] direction. This direction is not parallel to the wave vector \mathbf{Q} of an incommensurate spin-density wave (ISDW) in bulk Cr. In a [Cr(80 Å)/Sn(2 Å)] multilayer, only a commensurate antiferromagnetic (CAF) structure appears at 7 K. In a multilayer with 160-Å-thick Cr layers, on the other hand, the CAF and ISDW with \mathbf{Q} parallel to the [010] and [001] directions coexist at low temperatures. These results can be explained by the competition between the nesting at the Fermi surface, which tends to form ISDW's with \mathbf{Q} parallel to the $\langle 100 \rangle$ directions, and an interface effect in the (011) interfaces, which tends to enhance the magnetic moments of Cr at the interfaces.

DOI: 10.1103/PhysRevB.71.014414

PACS number(s): 75.70.-i, 75.25.+z, 75.30.Fv, 76.80.+y

I. INTRODUCTION

Chromium is an itinerant antiferromagnet and forms incommensurate spin-density waves (ISDW's) with the wave vector \mathbf{Q} along the bcc $\langle 100 \rangle$ directions below the Néel temperature 311 K in bulk state.¹ The formation of ISDW's is attributed to the nesting effect at the Fermi surface. The magnetic properties of pure Cr and Cr alloys in the bulk state were reviewed by Fawcett *et al.*^{1,2} Cr in multilayers shows a variety of magnetic structure due to proximity effects, as reviewed recently by Zabel,³ Pierce *et al.*⁴ and Fishman.⁵ However, in most of the multilayers, the magnetic structure of Cr at the interface region is not clarified experimentally.

Studies of the Cr magnetic structure in Cr(001)/Sn multilayers with ¹¹⁹Sn monatomic spacer layers have already been reported.⁶⁻⁸ In these multilayers, ¹¹⁹Sn Mössbauer spectroscopy was used to obtain information on the magnetism of Cr at the interfaces. In addition, neutron diffraction measurements gave information on the long-ranged magnetic ordering. The combination of these two methods allows us to discuss the relation between the interface effect and the magnetic order in the multilayers. ¹¹⁹Sn Mössbauer spectroscopy showed large hyperfine fields at Sn nuclear sites.^{6,8} It was confirmed theoretically that the large hyperfine fields are related to the enhancement of Cr magnetic moments at the interfaces.⁹ Neutron diffraction measurements proved that an ISDW is formed in the Cr layers at low temperatures when the Cr-layer thickness is equal to or thicker than 80 Å.^{7,8} The wave vector \mathbf{Q} is restricted to being parallel to the growth direction [001]. The wavelength of the ISDW is harmonic with the period of the superlattice and changes discretely as a function of the Cr-layer thickness. Taking into account the enhancement of Cr magnetic moments at the interfaces, this behavior can be attributed to a competition between the nesting effect at the Fermi surface and the boundary condition that pins antinodes of the ISDW at the interfaces.

We report here the spin structure of Cr layers in epitaxial Cr(011)/Sn multilayers. In these multilayers, monatomic Sn layers are periodically inserted along the bcc [011] direction, which is not parallel to \mathbf{Q} of the ISDW in bulk Cr. It was found from ¹¹⁹Sn Mössbauer spectroscopy that the interface effect that enhances the moments of Cr at the interfaces exists also in these multilayers.^{10,11} We show here how the periodic modulation of the composition along the [011] direction affects the magnetic structure of Cr layers. We carried out x-ray diffraction measurements to study the crystal structure of the multilayers and neutron diffraction measurements to investigate the magnetic ordering of the Cr layers.

II. EXPERIMENT

We have grown two epitaxial Cr(011)/Sn multilayers with different Cr-layer thicknesses using an ultrahigh-vacuum deposition technique. The first sample is MgO(111)/Cr(50 Å)/[Sn(2 Å)/Cr(80 Å)] \times 40. The MgO(111) substrate was chemically etched and introduced into a deposition chamber and annealed at 400 °C for 1 h. The buffer Cr layer was deposited at 200 °C, followed by the deposition of [Sn/Cr] layers at 400 °C. The second one is Al₂O₃(11 $\bar{2}$ 0)/Nb(100 Å)/Cr(50 Å)/[Sn(2 Å)/Cr(160 Å)] \times 20. The sapphire substrate was annealed for 1 h at 800 °C in the chamber. The Nb buffer layer was grown at 800 °C and the following layers at 400 °C.

To clarify the quality of the out-of-plane crystal structure and the periodicity, we performed x-ray diffraction measurements with the scattering vectors normal to the surface. To know the in-plane structure, we carried out measurements in which the scattering vector was fixed in plane and the angle ϕ , which corresponds to the rotation of the sample around the direction normal to the surface, was scanned. The former

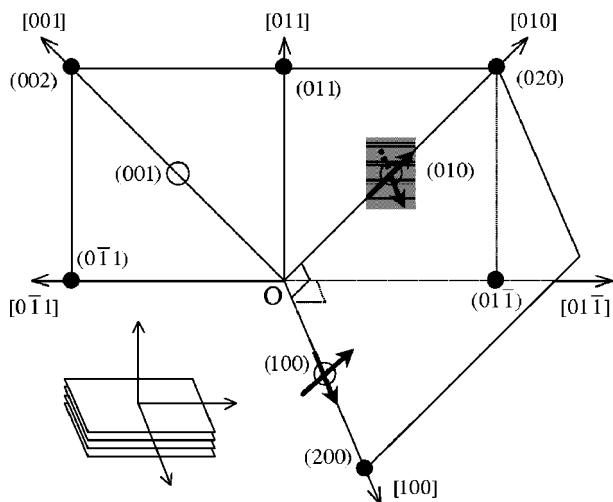


FIG. 1. Reciprocal lattice of Cr(011)/Sn multilayers. The contour map scan of neutron diffraction for the [Cr(80 Å)/Sn(2 Å)] multilayer was carried out at the shaded area. The position and direction of the line scans for the [Cr(160 Å)/Sn(2 Å)] multilayer are illustrated with arrows.

were carried out using Cu $K\alpha$ and the latter Cu $K\alpha_1$ radiation.

In order to make clear the magnetic structure of Cr layers, we carried out neutron diffraction measurements with a triple-axis spectrometer TOPAN at JRR-3M in JAERI. The incident neutron energy was fixed at 14.7 meV using a pyrolytic graphite (PG) (002) monochromator. A PG filter was employed to suppress the higher orders of incident neutrons. The structure factor in bcc crystals is zero at the reciprocal lattice points where the sum of the three indexes ($H+K+L$) is odd. Hence the diffraction peaks at these points are of pure magnetic origin. The existence of a commensurate antiferromagnetic (CAF) structure leads to a single peak at these points and that of the ISDW results in satellite peaks around these points. The positions of the satellite peaks are shifted along the wave vector \mathbf{Q} of the ISDW with the displacement δ , where $\delta=1-a|\mathbf{Q}|/2\pi$ and a is the lattice constant. The wavelength of the envelop curve of the modulation of moments in the ISDW is expressed as $\Lambda=a/\delta$. Figure 1 is a picture in the reciprocal space which shows the area of the contour map scan and the line scans at the Cr(010) and (001) points.

III. RESULTS

A. X-ray characterization

Out-of-plane x-ray diffraction patterns for the sample with 80-Å-thick Cr layers on the MgO(111) substrate are shown in Fig. 2(a). Satellite peaks appear around the Cr(011) peak, indicating that Cr and Sn grow epitaxially also in this orientation, although they have different crystal structures and different lattice constants in bulk states. The superlattice period of this sample deduced from the satellite peaks is 84.2 Å, while the nominal period is 82 Å. The grain size along the out-of-plane [011] direction deduced from the width of the Cr(011) fundamental peak in Fig. 2 is 400 Å. The result of

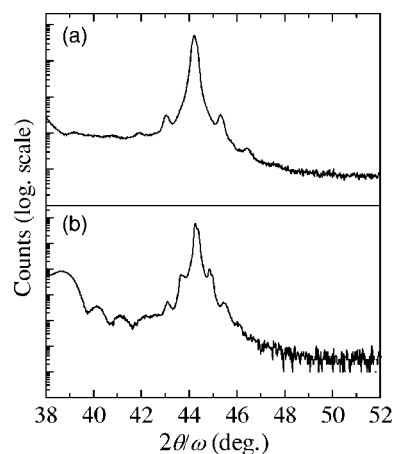


FIG. 2. X-ray out-of-plane $2\theta/\omega$ scans for (a) [Cr(80 Å)/Sn(2 Å)] and (b) [Cr(160 Å)/Sn(2 Å)] multilayers.

an in-plane ϕ scan for Cr(200) of this sample is shown in Fig. 3(a), indicating that three crystallographic domains co-exist which are directed with an angle of 120° to each other. The in-plane relationship of the Cr(011) and MgO(111) planes is equal to that reported by Mattson *et al.*¹²

Figure 2(b) exhibits the x-ray diffraction patterns for the sample with 160-Å-thick Cr layers on the $\text{Al}_2\text{O}_3(11\bar{2}0)$ substrate. The artificial period deduced from the satellite peaks is 159 Å, while the nominal period is 162 Å. The grain size is estimated to be 1000 Å. Figure 3(b) shows the pattern of the in-plane ϕ scan for the Cr(200) peaks. This pattern means that there are two domains and the volume of the minority domain is about a hundredth of that of the majority domain. The in-plane relation in the reciprocal space between the $\text{Al}_2\text{O}_3(11\bar{2}0)$, Nb(011), and Cr(011) planes is depicted in Fig. 4. This relation between sapphire and the majority domain is equal to that reported by Sonntag *et al.*¹³

B. Neutron diffraction measurement

Neutron diffraction measurements were performed for the largest domain deduced from the x-ray ϕ scans in each

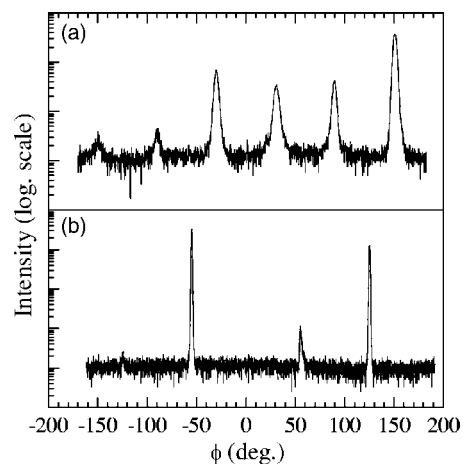


FIG. 3. In-plane ϕ scans of the Cr(200) peaks in (a) MgO(111)/[Cr(80 Å)/Sn(2 Å)] and (b) $\text{Al}_2\text{O}_3(11\bar{2}0)$ /[Cr(160 Å)/Sn(2 Å)] multilayers. The angle ϕ is measured relative to MgO[$2\bar{1}\bar{1}$] for (a) and Al_2O_3 [0001] for (b).

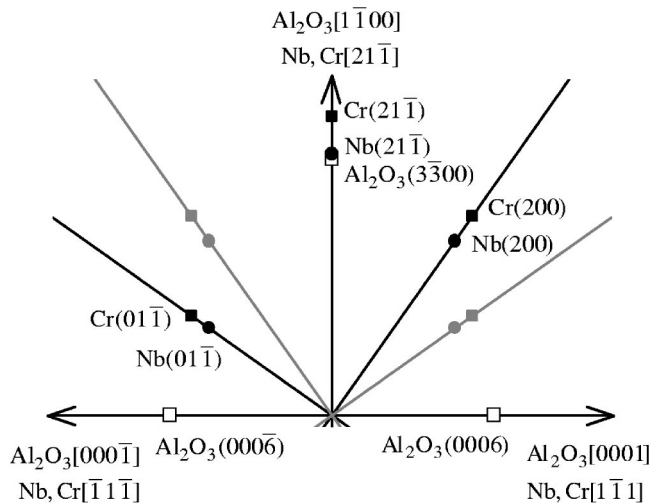


FIG. 4. In-plane relation of $\text{Al}_2\text{O}_3(11\bar{2}0)$, $\text{Nb}(011)$, and $\text{Cr}(011)$ planes in the reciprocal space for $\text{Al}_2\text{O}_3(11\bar{2}0)/[\text{Cr}(160 \text{ \AA})/\text{Sn}(2 \text{ \AA})]$ multilayer. The open squares represent Al_2O_3 points. The solid circles and squares represent Nb and Cr, respectively; the black points correspond to the majority domains of Nb and Cr and the gray points minority domains.

sample. The contour map at 7 K for the shaded area in Fig. 1 of the $[\text{Cr}(80 \text{ \AA})/\text{Sn}(2 \text{ \AA})]$ multilayer is shown in Fig. 5(a). Line profiles at 10 K through the $\text{Cr}(010)$ point parallel to the $[010]$ and $[001]$ directions are shown in Figs. 5(b) and 5(c), respectively. Weak powder patterns from the sample holder appear in the contour map and the line profile (b), and no satellite peak is observed in Figs. 5(a)–5(c), indicating that only the CAF structure is stabilized and the ISDW does not appear at low temperatures. This is in contrast with the $\text{Cr}(001)/\text{Sn}$ multilayer with the same Cr layer thickness, where the ISDW is stabilized at low temperatures.

In the case of the $[\text{Cr}(160 \text{ \AA})/\text{Sn}(2 \text{ \AA})]$ multilayer, the situation is different. Shown in Fig. 6 is the result of line profiles through the $\text{Cr}(100)$ point and parallel to $[010]$ at several temperatures. In these patterns, satellite peaks appear below 200 K, and a peak at the $\text{Cr}(100)$ point still exists. This means that both domains of CAF structure and ISDW with \mathbf{Q} parallel to $[010]$ exist. An ISDW with \mathbf{Q} parallel to $[001]$ is also expected to exist, since in this multilayer, $[010]$ and $[001]$ are equivalent. This result is in contrast to that of a $\text{Cr}(001)/\text{Sn}$ multilayer with 160-Å-thick Cr layers, in which only the ISDW is observed at low temperatures.⁸ The magnitude of \mathbf{Q} at each temperature is shown in Fig. 7. The obtained values are larger than the bulk value which increases as the temperature increases and reaches the value of 0.963 in units of $2\pi/a$ at Néel temperature.¹⁴ In $\text{Cr}(001)/\text{Sn}$ multilayers with Cr layers thicker than 80 Å, the wavelength does not depend on temperature due to the pinning of the antinodes of the ISDW at the interfaces. Note that samples with a specific Cr-layer thickness show a discrete change of the wavelength when temperature changes, which corresponds to a change of number of nodes in the Cr layers.¹⁵ From Fig. 7 for the $\text{Cr}(011)/\text{Sn}$ multilayer, it is not clear whether the wavelength is constant or not.

We also performed scans with the scattering vector parallel to the in-plane $[100]$ direction across both $\text{Cr}(010)$ and

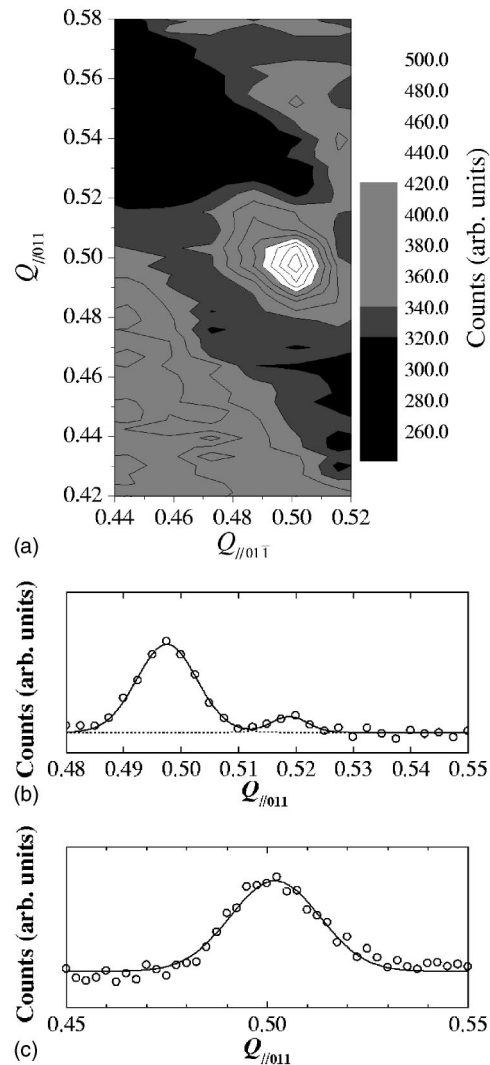


FIG. 5. (a) Contour map of the neutron diffraction intensity at 7 K of the $[\text{Cr}(80 \text{ \AA})/\text{Sn}(2 \text{ \AA})]$ multilayer for the gray area in the reciprocal space in Fig. 1. $Q_{\parallel 011}$ is parallel to the out-of-plane $[011]$ direction and defined in units of $2\pi/d_{011}$, and $Q_{\parallel 01\bar{1}}$ is parallel to the in-plane $[01\bar{1}]$ direction and is defined in units of $2\pi/d_{01\bar{1}}$. The $(0.5, 0.5)$ point corresponds to the $\text{Cr}(010)$ point. The base intensity in the scanned area is 260 counts in arbitrary units. (b) (c) Line profiles at 10 K through the $\text{Cr}(010)$ point parallel to the $[010]$ and $[001]$ directions, respectively. Note that weak powder patterns from the sample holder appear in the contour map and the line profile (b).

(100) points for $\text{Cr}(011)/\text{Sn}$ with 160-Å-thick Cr layers (shown in Fig. 1), so that we could investigate the existence of both transverse and longitudinal ISDW's with \mathbf{Q} along the in-plane $[100]$ direction. In the obtained patterns at 8 K shown in Fig. 8, only a single peak appears, revealing that no ISDW with \mathbf{Q} parallel to the in-plane $[100]$ direction exists even at 8 K. The ISDW with in-plane \mathbf{Q} is not observed for the $\text{Cr}(001)/\text{Sn}$ multilayers, either.^{7,8,15}

IV. DISCUSSION

We propose here an explanation for the obtained results considering the interface effect. We first discuss the result of

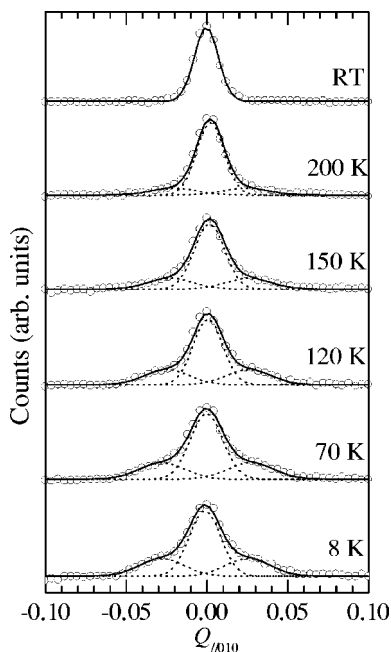


FIG. 6. Neutron diffraction patterns around the Cr(100) point along the [010] direction for the [Cr(160 Å)/Sn(2 Å)] multilayer. $Q_{//010}$ is defined as being parallel to [010] and expressed in units of $2\pi/d_{010}$. The results of Gaussian fitting are drawn with lines.

the [Cr(160 Å)/Sn(2 Å)] multilayer. It has both CAF structure and ISDW at low temperatures, and Q of the ISDW is parallel to the [010] or [001] direction, which are shifted by 45° from the [011] direction normal to the surface. In a Cr(001)/Sn multilayer with the same Cr-layer thickness the ISDW with Q parallel to the out-of-plane [001] direction is stabilized and the wavelength is harmonic with the artificial period and longer than that of bulk Cr. This magnetic structure is determined by two factors: one is the nesting effect at the Fermi surface which tends to make planes of antinodes parallel to $\{100\}$ planes, and the other is the interface effect which behaves as a boundary condition located in the (001) interfaces. These factors result in a magnetic structure in which the ISDW with Q parallel to [001] changes its wavelength and some of the (001) planes of antinodes are located on the interfaces. ^{119}Sn Mössbauer spectra at room tempera-

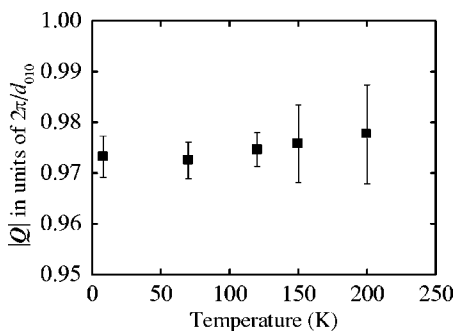


FIG. 7. Temperature dependence of the magnitude of the wave vector Q of the ISDW deduced from the neutron diffraction patterns in Fig. 6. $|Q| = 2\pi(1 - \delta)/d_{010}$, where δ is the incommensurability of the ISDW.

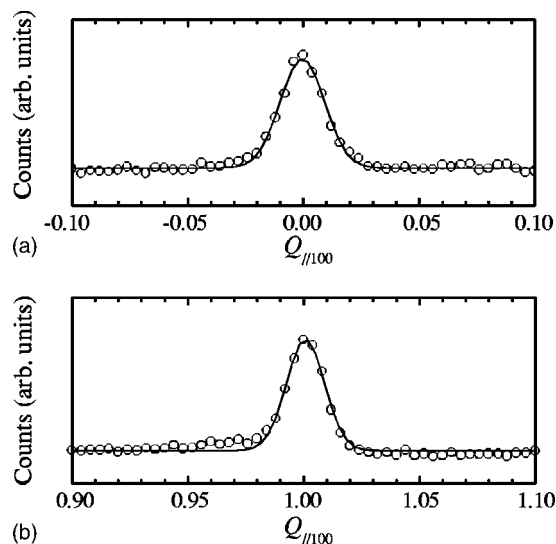


FIG. 8. Neutron diffraction pattern at 8 K for a [Cr(160 Å)/Sn(2 Å)] multilayer along the in-plane [100] direction across (a) the Cr(010) point and (b) the Cr(100) point. $Q_{//100}$ is in units of $2\pi/d_{100}$.

ture of not only the Cr(001)/Sn multilayers but also the Cr(011)/Sn multilayers show an enhancement of Cr magnetic moments near the interfaces.^{10,11} Therefore, also in the Cr(011)/Sn multilayer, the antinodes of the ISDW might be expected to be pinned at the interfaces and the wavelength extended. In fact, the obtained wavelength of the ISDW is longer than the bulk value. However, we have to consider that the two factors are incompatible in this orientation. The interface which behaves as a boundary located in the (011) planes can not be parallel to any of the planes of antinodes $\{100\}$ coming from the nesting effect. If the boundary condition is so strong as to prohibit ISDW's lying across the interfaces, both CAF structure and ISDW are formed as observed in our experiment: the antinodes of the ISDW are pinned at a depth close to but a little apart from the interfaces and CAF structure exists at the interfaces. A simple picture of the magnetic structure of Cr in this multilayer is depicted in Fig. 9. The size of the ISDW domains along their Q is in principle estimated from the peak widths in the neutron diffraction pattern at the (010) point along the [010] direction. However, the estimation was not possible because the peak widths were comparable to the resolution limit of our neutron diffraction setup.

The ISDW with in-plane Q is not observed at 8 K. This is also the case in the Cr(001)/Sn multilayers. These facts common for both multilayers can also be explained by the enhancement of Cr magnetic moments near the interfaces. If an in-plane ISDW exists, there must be both nodes and antinodes near the interfaces. We speculate that the interface effect enhances the Cr magnetic moments and suppresses the ISDW with in-plane Q .

In the [Cr(80 Å)/Sn(2 Å)] multilayer, only CAF structure is stabilized down to 7 K. This result is different from that of the Cr(011)/Sn multilayer with 160-Å-thick Cr. This behavior can be explained as follows. The boundary condition is located in the planes at an angle of 45° to the nesting direc-

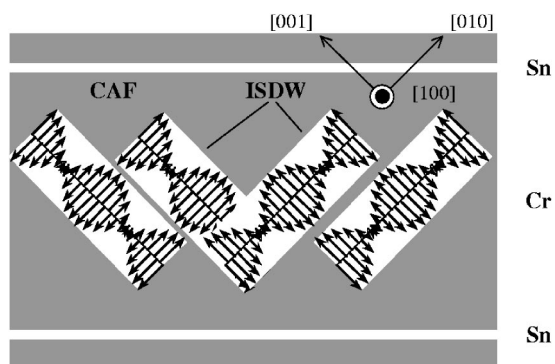


FIG. 9. Simple picture of the magnetic structure in a $[\text{Cr}(160 \text{ \AA})/\text{Sn}(2 \text{ \AA})]$ multilayer. Both domains of the ISDW and CAF structure coexist in Cr layers below 200 K. The ratio of volume between transverse and longitudinal ISDW's is not clear.

tions $[010]$ and $[001]$. The ISDW cannot go through the interfaces and the CAF structure is stabilized around the interfaces. Then, when the Cr layers are thin, the middle part of the Cr layers is not thick enough for the formation of an ISDW, so that the CAF structure is stabilized in the whole Cr layers. The in-plane grain sizes of the Cr crystals in the $[\text{Cr}(80 \text{ \AA})/\text{Sn}(2 \text{ \AA})]$ multilayer are small because of the existence of the three equivalent domains, and we cannot deny that this is the reason for the suppression of the ISDW in this multilayer.

Fritzsche *et al.* investigated the SDW of Cr layers in a $[\text{Fe}(120 \text{ \AA})/\text{Cr}(260 \text{ \AA})]$ multilayer with bcc (011) orientation,¹⁶ where the Cr layers are thicker than those in the present study. They found that the ISDW with $\mathbf{Q} \parallel [010]$ and $[001]$ is stabilized without CAF structure below 175 K. Our ¹¹⁹Sn Mössbauer measurements for Sn layers in Cr layers of $\text{Fe}(011)/\text{Cr}$ multilayers^{10,11} suggest that the boundary

condition at the Fe/Cr interface tends to reduce the magnetic moments of Cr layers around the interfaces. This is due to a large magnetic frustration which comes from the proximity of a magnetically compensated Cr(011) layer and a ferromagnetic Fe(011) layer. Hence, we expect that only the ISDW with nodes around the interfaces is stabilized in the middle of the Cr layers.

V. CONCLUSION

We have investigated the magnetic structures of the Cr layers in $\text{Cr}(011)/\text{Sn}$ multilayers. The interface effect at the Cr/Sn interfaces, which enhances the magnetic moments of Cr, behaves as a boundary condition for the magnetic order in the Cr layers. This boundary condition is incompatible with the nesting effect which tends to form ISDW's with the planes of antinodes in the $\{100\}$ planes, resulting in a separation of a Cr layer into two types of magnetic domains in the $[\text{Cr}(160 \text{ \AA})/\text{Sn}(2 \text{ \AA})]$ multilayer. One is CAF structure which is located around the interface. The other is the ISDW which is stabilized in the middle of the Cr layers with the antinodes pinned near the interfaces. When the Cr-layer thickness is smaller and the middle part of the Cr layers is not long enough for the formation of a long modulation of the ISDW, all parts of the Cr layers consist of CAF structure, as observed in the $[\text{Cr}(80 \text{ \AA})/\text{Sn}(2 \text{ \AA})]$ multilayer.

ACKNOWLEDGMENTS

This work was partially supported by Grants-in-Aid for COE Research ("Elements Science") from the Ministry of Education, Culture, Sports, Science, and Technology of Japan and Scientific Research (C) from the Japan Society for the Promotion of Science.

*Electronic address: jiko@ssc1.kuicr.kyoto-u.ac.jp

¹E. Fawcett, *Rev. Mod. Phys.* **60**, 209 (1988).

²E. Fawcett, H. L. Alberts, V. Y. Galkin, D. R. Noakes, and J. V. Yakhmi, *Rev. Mod. Phys.* **66**, 25 (1994).

³H. Zabel, *J. Phys.: Condens. Matter* **11**, 9303 (1999).

⁴D. T. Pierce, J. Unguris, R. J. Celotta, and M. D. Stiles, *J. Magn. Magn. Mater.* **200**, 290 (1999).

⁵R. S. Fishman, *J. Phys.: Condens. Matter* **13**, R235 (2001).

⁶K. Mibu, S. Tanaka and T. Shinjo, *J. Phys. Soc. Jpn.* **67**, 2633 (1998).

⁷M. Takeda, K. Mibu, K. Takanashi, K. Himi, Y. Endoh, T. Shinjo, and H. Fujimori, *J. Phys. Soc. Jpn.* **69**, 1590 (2000).

⁸K. Mibu, M. Takeda, J. Suzuki, A. Nakanishi, T. Kobayashi, Y. Endoh, and T. Shinjo, *Phys. Rev. Lett.* **89**, 287202 (2002).

⁹H. Momida and T. Oguchi, *J. Magn. Magn. Mater.* **234**, 126

(2001).

¹⁰N. Jiko, M. Almokhtar, T. Shinjo, M. Takeda, J. Suzuki, and K. Mibu, *J. Magn. Magn. Mater.* **272–276**, 1233 (2004).

¹¹N. Jiko, M. Almokhtar, K. Mibu, and T. Shinjo (unpublished).

¹²J. E. Mattson, E. E. Fullerton, C. H. Sowers, and S. D. Bader, *J. Vac. Sci. Technol. A* **13**, 276 (1995).

¹³P. Sonntag, W. Donner, N. Metoki, and H. Zabel, *Phys. Rev. B* **49**, 2869 (1994).

¹⁴S. A. Werner, A. Arrott, and H. Kendric, *Phys. Rev.* **155**, 528 (1967).

¹⁵M. Takeda, K. Mibu, T. Shinjo, Y. Endoh, and J. Suzuki, *Phys. Rev. B* **70**, 104408 (2004).

¹⁶H. Fritzsche, S. Bonn, J. Hauschild, J. Klenke, K. Prokes, and G. J. McIntyre, *Phys. Rev. B* **65**, 144408 (2002).